International Scientific Publications: Materials, Methods and Technologies, Vol. 2
ISSN 1313-2539

RESEARCH OF VIBRATIONS ACTING THE COMPARATORS CARRIAGE

Arturas Kilikevichus[1], Vladas Vekteris [2]

[1, 2] Vilnius Gediminas Technical University, Department of Machine building, Basanaviciaus str. 28, Vilnius, Lithuania

Abstract

Oscillations of the comparator, which is used for the dynamic calibration of long optical line scales, are analyzed in the paper. The accuracy of determination of the position of optical lines on the scale depends on the velocity of the carriage, which transports the microscope with a CCD camera in relation to the line scale. Oscillations influence the velocity equability, its value, and at the same time the error compo measuring. The base part of the comparator is acted upon by external excitations which come through the foundation and supports, also due to natural frequencies of the comparator set. It is shown in the work that vibration surroundings acting on the comparator have a random character and correspond to the criteria of the normal (Gauss) distribution. It is proved experimentally that preaching amplitudes of measured components of vertical and horizontal oscillations influence the stability of the carriage movement which causes the error of measuring.

Key words: *comparator, dynamic calibration, vibration, carriage, measuring, calibrated scale.*

1. INTRADUCTION

Line gauges are important components in the length link chain. They are used in the measuring devices (systems) and technological equipment, etc.

The world practice witnesses increased focusing on the improvement of line gauge technologies and application thereof in length measurement and precise controlled motion systems. Modern precision scale production technologies enable to create small-step displacement transducers with measuring possibilities that come close to those of optical interferometers. Currently, line gauges with 0,125 nm (1,25 Å) resolution are used in precision devices [1, 2, 3].

A rapid advance of technologies, primarily micro- and nanotechnologies as well as micro-electro-mechanical system (MEMS) technologies raises higher and higher precision requirements, measuring speed requirements and other requirements thus stimulating creation of new precision length calibration systems. Reacting to these challenges the national metrology institutes (NMI) and manufacturing companies create new linear scale comparators whereof calibration uncertainty is a value of the nanometer range.

A line gauge defines one or several length values which are determined by the shortest distance between the centers of two lines of the periodic structure (scale).

Line gauges are calibrated by means of optical interference comparators with a sliding microscope for viewing scale lines and with a sliding measuring scale [4-6]. Interferometric measuring systems are used for precise measurement of the displacement of these sliding parts. Generally, the sources of interferometer stabilized frequency radiation are double-frequency He-Ne lasers.

A calibrated scale is precisely exposed under the microscope. Split-field photoelectric microscopes, point projection microscopes, confocal microscopes and photoelectric microscopes with CCD camera are used for the initial positioning and the positioning of the centers of lines of the measuring scale. The type of the microscope used determines in essence the measurement signal processing algorithm and

ISSN 1313-2539

the calibration precision and rate. Further details about line (edge) detection microscopes are presented in [4, 6].

Besides many device characteristics whereon scanning of line gauges of the comparator is dependent, external factors affect the precision of the device as well. One of the utmost effects is produced by vibrations. Lengthwise vibrations affect the carriage speed dynamics which directly affects the scanning precision.

The length of the calibrated end gauge and the position of line centers are precisely determined (calculated) by processing of the measurement data, by estimating the corrections of the environment conditions on the basis of pressure, humidity, temperature and CO_2 content measurement results. The lengths of the scale intervals obtained from the measuring system are recalculated for the 20 °C temperature.

The line gauge calibration procedures are determined by documents [7, 8-13].

The impact of vibrations on the precision of calibration of line gauges is discussed in this paper.

Most dangerous are the vibrations that occur in the direction of the carriage motion (x axis) and torsional vibrations that occur on the carriage axis z (on x, y plane) which is perpendicular to the direction of motion x. Vibrations that occur in the direction of the length of the carriage, i.e. the carriage velocity and its dynamics determine the precision of scanning of the line gauge position. Precision is defined by means of a photoelectric microscope with a CCD camera. Torsional vibrations cause an error specified in Fig. 1.

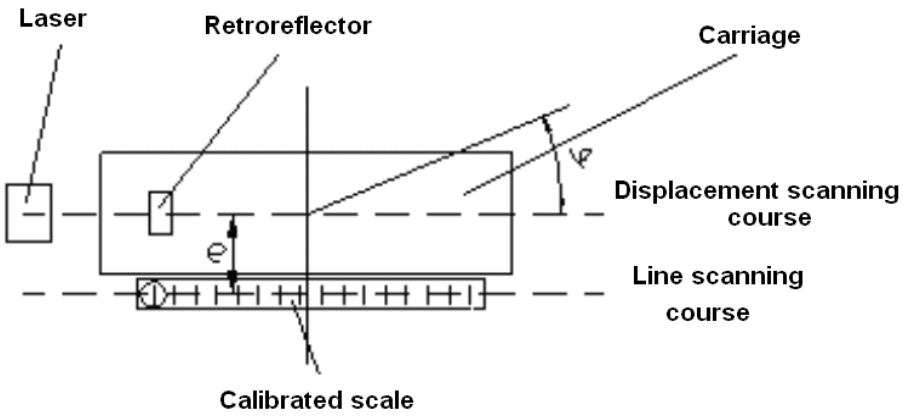


Fig. 1. Angular vibration error

When the device displacement measurement system is parallel to the measuring direction and is distanced from it by length *e*, Abbe's error occurs:

$$\Delta = \varphi \cdot e. \tag{1}$$

The carriage speed will be equal to:

$$v = v_{a.} + \delta_l + \delta_\varphi \tag{2}$$

$v_{a.}$ – actual, assigned speed;

δ_l – speed change due to lengthwise vibrations;

ISSN 1313-2539

δ_φ – speed change due to angular vibrations.

Thus, the dangerous speed error (3) will be created by the function of speed changes that occur due to lengthwise and angular vibrations:

$$\Delta v = f\left(\delta_l + \delta_\varphi\right) \quad (3)$$

2. OBJECT OF RESEARCH

An interference comparator with air refraction coefficient compensation meets the technical and economic criteria by estimating the refraction coefficient from Edlen formula according to the results of measurement of the environment parameters or by means of a refractometer. The structural diagram of the equipment is shown in Fig. 2. It is based on a line gauge calibration comparator with a sliding microscope and a stationary scale. The comparator's frameis made from granite and is mounted on vibration-proof supports, the microscope holder moves on air guides. The carriage is driven by means of motor, worm reduction gear and friction gear. T, P and H are temperature, pressure and humidity meters, respectively. The laser measuring system comprises laser, interferometer and retroreflector. Letters A, B, and C show the measurement points.

The position of line centers of the calibrated gauge is precisely determined (calculated) by processing the measurement data and estimating corrections for geometrical, instrumental and environmental errors.

The comparator is installed in a standard (conditioned) room.

The whole operation of the comparator and error compensation are computer-controlled.

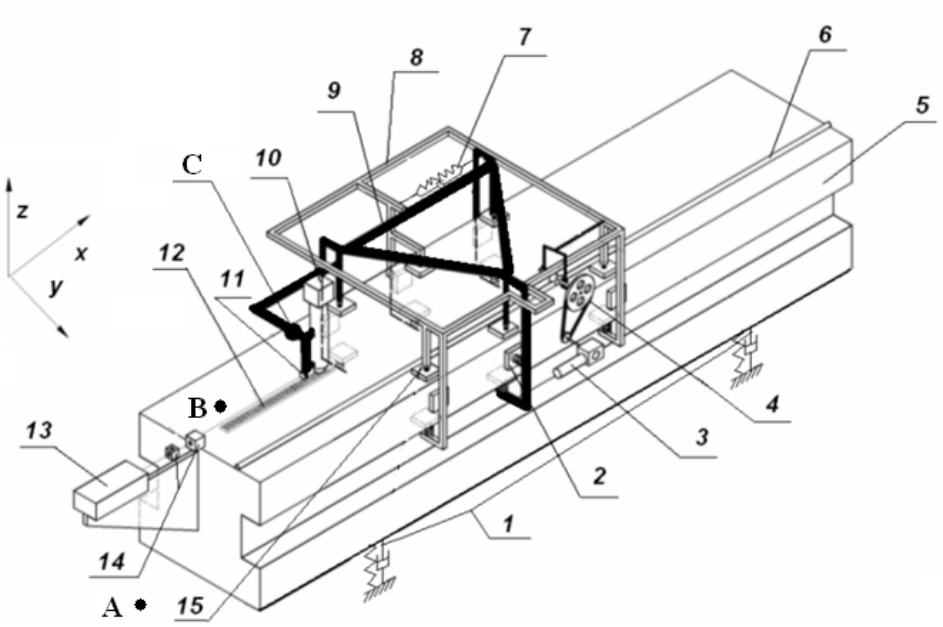


Fig.2. A structural diagram of the comparator: 1 – vibration insulation supports; 2 – springy aerostatic bearing; 3 – electromotor with reducer; 4 – belt drive; 5 – granite guideway; 6 – friction gear; 7 – joint member of two carriage; 8 – frame of force carriage; 9 – frame of the precision carriage; 10 – microscope with camera and flash; 11 – retroreflektor; 12 – calibrate scale; 13 – laser head; 14 – linear interferometer; 15 –tight built aerostatic bearing, A, B, and C – measurement points.

ISSN 1313-2539

3. DYNAMICAL MODEL OF THE COMPARATOR

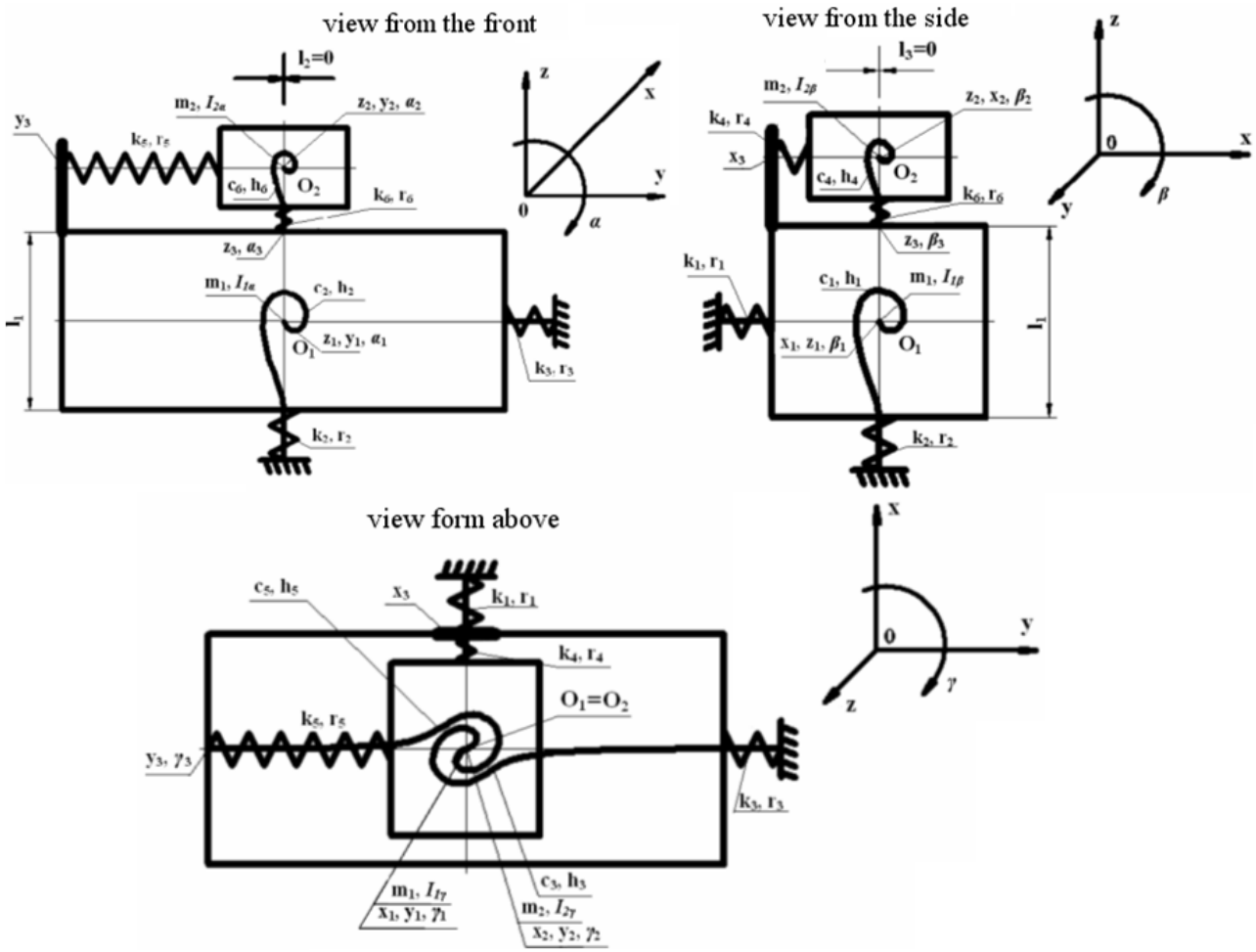


Fig.3. Dynamical model of the comparator

There O_1, O_2 – center of masses; m_1, m_2 – are masses of assembly units; I_{1j}, I_{2j}, inertia moments, where j – coincides with angles α, β, γ;

Stiffness coefficients k_n – is of linear motion; c_n – is of angular rotation motion (n=1,..., 6). Damping coefficients r_n – is of linear motion; h_n – is of angular rotation motion (n=1,...,6).

For equation forming simplification the dynamic model at a comparator we are dividing into two subsystems: the 1–st subsystem consists of vibration insulation supports without connection with a carriage; the 2–nd subsystem consists of carriage with ties connecting it with the bed of granite.

The main coordinates of two subsystem are x_i, y_i, z_i, α_i, β_i, γ_i (i=1, 2) which fix linear and angular motions of mass centers in coordinate systems with initial position in points O_1 and O_2. All members of coordinates are 12 main ones and 6 additional: x_3, y_3, z_3, α_3, β_3, γ_3.

To research vibration of 12 degree of freedom systems is mostly compact at using matrices. A vibration of the system is mostly convenient to describe by matrix:

$$[A]\{\ddot{q}\}+[B]\{\dot{q}\}+[D]\{q\}=\{Q(t)\} \qquad (4)$$

ISSN 1313-2539

There [*A*], [*B*], [*D*] are generalized inertia, damping and stiffness coefficients of matrices; $\{q\}$, $\{\dot{q}\}$, $\{\ddot{q}\}$ are generalized coordinates of displacement, velocity and acceleration one columns matrices; $\{Q(t)\}$ – external generalized force column acting in accordance with force:

$$[A]=\begin{bmatrix} a_{11} & a_{12} & \dots & a_{112} \\ a_{21} & a_{22} & \dots & a_{212} \\ \vdots & \vdots & \vdots & \vdots \\ a_{121} & a_{122} & \dots & a_{12,12} \end{bmatrix};\quad [B]=\begin{bmatrix} b_{11} & b_{12} & \dots & b_{112} \\ b_{21} & b_{22} & \dots & b_{212} \\ \vdots & \vdots & \vdots & \vdots \\ b_{121} & b_{122} & \dots & b_{12,12} \end{bmatrix};\quad [D]=\begin{bmatrix} d_{11} & d_{12} & \dots & d_{112} \\ d_{21} & d_{22} & \dots & d_{212} \\ \vdots & \vdots & \vdots & \vdots \\ d_{121} & d_{122} & \dots & d_{12,12} \end{bmatrix} \tag{5}$$

$$\{q\}=\begin{Bmatrix} q_1 \\ q_2 \\ \vdots \\ q_{12} \end{Bmatrix};\quad \{\dot{q}\}=\begin{Bmatrix} \dot{q}_1 \\ \dot{q}_2 \\ \vdots \\ \dot{q}_{12} \end{Bmatrix};\quad \{\ddot{q}\}=\begin{Bmatrix} \ddot{q}_1 \\ \ddot{q}_2 \\ \vdots \\ \ddot{q}_{12} \end{Bmatrix};\quad \{Q(t)\}=\begin{Bmatrix} Q_1(t) \\ Q_2(t) \\ \vdots \\ Q_{12}(t) \end{Bmatrix} \tag{6}$$

Expression at kinetic and potential energy and dissipative function it is possible to write as a product of row matrix and one columns matrix:

$$T=\frac{1}{2}\{\dot{q}\}^T[A]\{\dot{q}\};\quad \Pi=\frac{1}{2}\{q\}^T[D]\{q\};\quad \Phi=\frac{1}{2}\{\dot{q}\}^T[B]\{\dot{q}\}; \tag{7}$$

There [*A*], [*B*], [*D*] are generalized inertia, damping and stiffness coefficients square 12 members matrix; $\{q\}$, $\{\dot{q}\}$ are one columns matrices and their differential; $\{q\}^T$, $\{\dot{q}\}^T$ are one row matrices of generalized coordinates and their differential.

When a dynamic model is obtained (Fig. 3) a mathematical model of the tested system is created (vibration equation). To this end Lagrange's equation of the second type is used [9]:

$$\frac{d}{dt}\left(\frac{dT}{d\dot{q}_i}\right)-\frac{dT}{dq_i}+\frac{d\Phi}{d\dot{q}}+\frac{d\Pi}{dq_i}=Q_i(t) \tag{8}$$

There T, Π are the system's kinetic and potential energy;

Φ – dissipation function;

q_i – i-th generalized coordinate;

$Q_i(t)$ – generalized force acting in accordance with coordinate q_i.

At forming of equation lat we use expressions of T_i and Π_i (i=1, 2) presented in formula 6.

ISSN 1313-2539

$$2T_i = m_i\left(\dot{x}_i^2 + \dot{y}_i^2 + \dot{z}_i^2\right) + I_{i\alpha}\dot{\alpha}_i^2 + I_{i\beta}\dot{\beta}_i^2 + I_{i\gamma}\dot{\gamma}_i^2; \quad (i = 1, 2)$$

$$2\Pi_1 = k_1(x_1 - x_0)^2 + k_3(y_1 - y_0)^2 + k_2(z_1 - z_0)^2 + c_2(\alpha_1 - \alpha_0)^2 + c_1(\beta_1 - \beta_0)^2 + c_3(\gamma_1 - \gamma_0)^2 \qquad (9)$$

$$2\Pi_2 = k_4(x_2 - x_3)^2 + k_5(y_2 - y_3)^2 + k_6(z_2 - z_3)^2 + c_5(\alpha_2 - \alpha_3)^2 + c_4(\beta_2 - \beta_3)^2 + c_6(\gamma_2 - \gamma_3)^2$$

There x_0, y_0, z_0, α_0, β_0, γ_0 are excitations of a bed with consequent coordinates. View at dissipation function (Φ_i) is received from Π_i, after changing stiffness coefficients to damping coefficients. Connecting equations are expressed:

$$x_3 - x_1 - l_1\beta_1 - l_2\gamma_2 = 0;\ y_3 - y_1 - l_1\alpha_1 - l_3\gamma_1 = 0;\ z_3 - z_1 - l_2\alpha_1 + l_3\beta_1 = 0;\ \alpha_3 - \alpha_1 = 0;\ \beta_3 - \beta_1 = 0;\ \gamma_3 - \gamma_1 = 0; \qquad (10)$$

After performing modeling by means of Matlab 6.1 and Origin 6.1 software packages we obtain the results presented in Fig. 4.

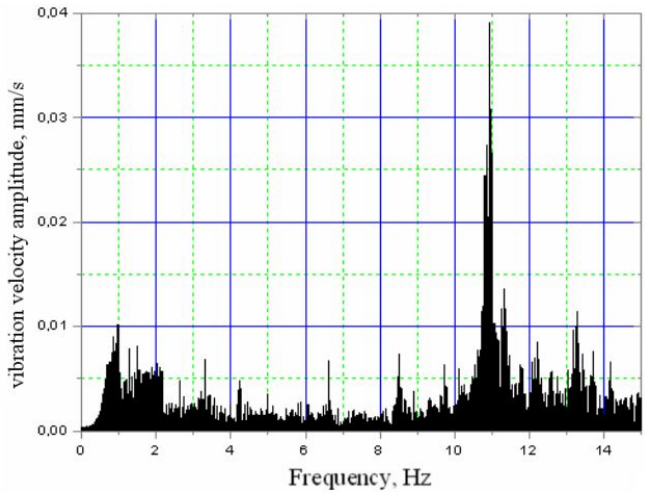


Fig.4. Point C, the spectrum of the vibration velocity (during dynamic calibration)

4. EXPERIMENTAL TESTS

Experimental tests were conducted in measurement paint shown in Fig. 5. The vibration measuring devices of the Denmark firm "Brüel & Kjær", with accelerometer 8306, vibrometer 2511, signal input and control board "Ebiol–Comlab–SeiTech" and personal computer IBM–50 was used for measuring of vibration parameters.

It was determinate during experimental investigation that dominated amplitudes of vertical and horizontal oscillations are comparatively of law frequencies (1–50Hz).

ISSN 1313-2539

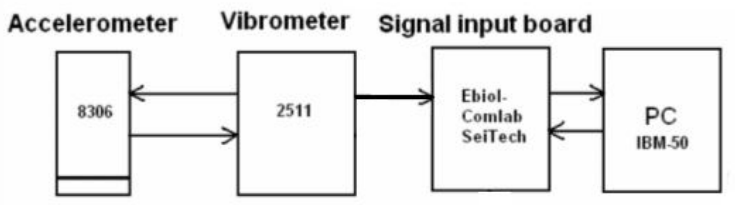


Fig.5. Flow chart of diagnostic measurements

In this paper was measured the vibration displacement and the vibration velocity. Measurement points A, B and C results in a static position are shown in Figures from 6 to 13. Results of measurement points C obtained during dynamic calibration are shown in Figures 14 and 15. Specters, distributions and statistic parameters of signals were calculated:

Arithmetic mean x, mm/s: $\bar{x} = \frac{1}{n}\sum_{i=1}^{n} x_i$;

Root mean square deviation: $S_X = \sqrt{\frac{1}{n-1}\sum_{i=1}^{n}\left(x_i - \bar{x}\right)^2}$;

Scatter: $x_{scatter} = \left|x_{\max}\right| + \left|x_{\min}\right|$.

There n is the number of measurement results, x – measurement result.

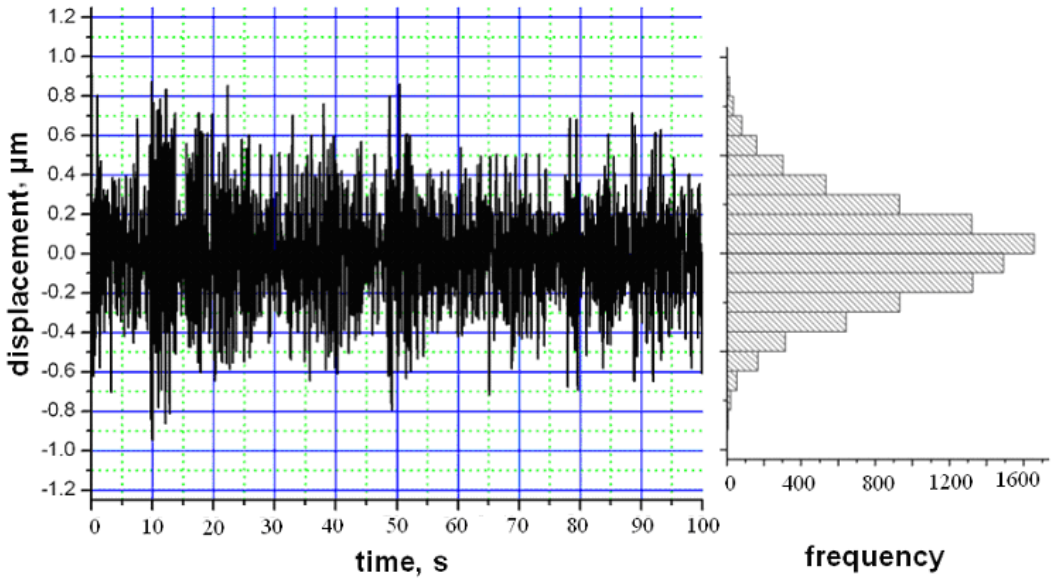


Fig. 6. Typical the signal of the displacement and its histogram

ISSN 1313-2539

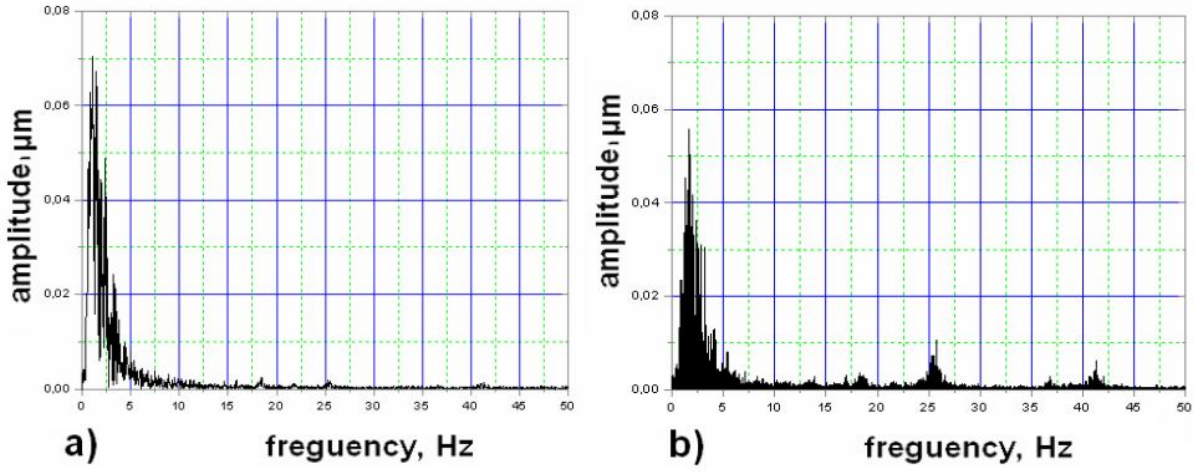


Fig.7. The spectrum of the displacement amplitude point A: a) horizontal direction, b) vertical direction.

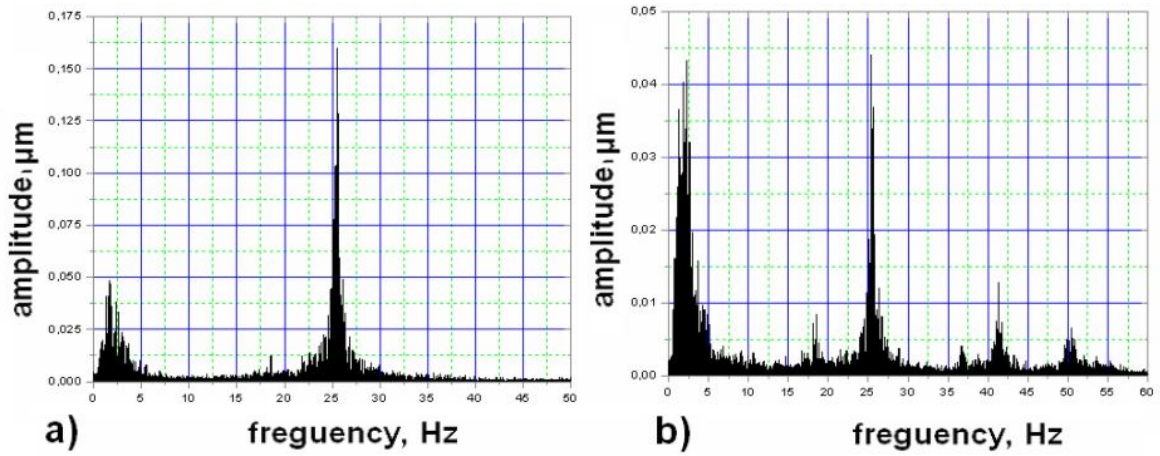


Fig.8. The spectrum of the displacement amplitude point B: a) horizontal direction, b) vertical direction.

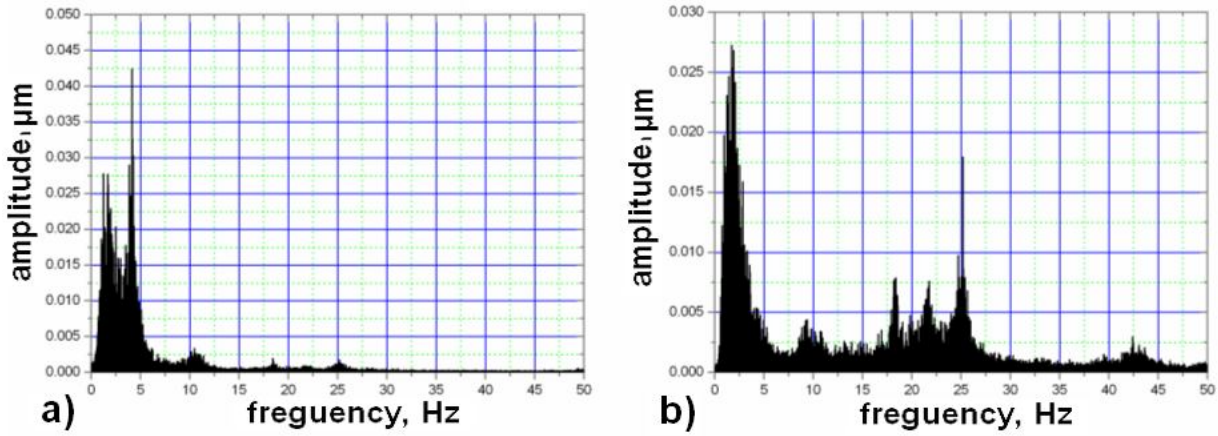


Fig.9. The spectrum of the displacement amplitude point C: a) horizontal direction, b) vertical direction.

ISSN 1313-2539

Table 1 Statistical parameters of the displacement measurement signal

Statistical parameter	Direction	Arithmetical mean, [mm/s]	Root mean square deviation	Minimum value, [mm/s]	Maximum value, [mm/s]	Scatter, [mm/s]
Point A	horizontal	2,348E-6	0,315	0,00315	-1,198	1,743
Point B	horizontal	0,0359	0,429	0,00429	-1,092	1,253
Point C	horizontal	-1,049E-6	1,258	0,0095	-4,241	3,775
Point A	vertical	-4,396E-6	0,211	0,00211	-0,905	0,817
Point B	vertical	4,711E-6	0,205	0,002	-0,762	0,746

The measurement point C with the precision carriage being in a static position (without air supplying).

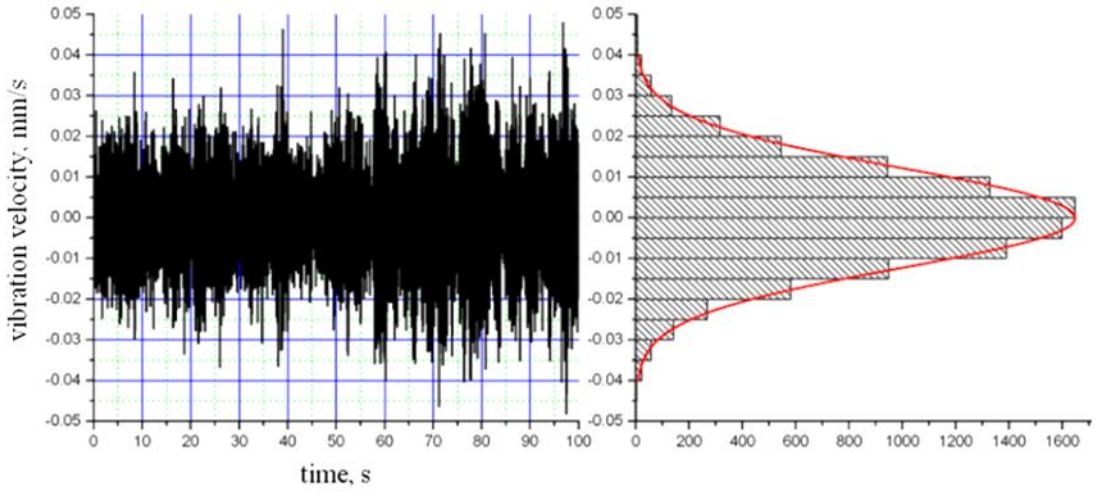


Fig.10. The signal of the vibration velocity and its histogram

Table 2 Statistical parameters of the vibration velocity measurement signal

Statistical parameter	Direction	Arithmetical mean, [mm/s]	Root mean square deviation	Minimum value, [mm/s]	Maximum value, [mm/s]	Scatter, [mm/s]
Point C	horizontal	-3.123E-6	0.01224	-0.04807	0.04795	0.09601

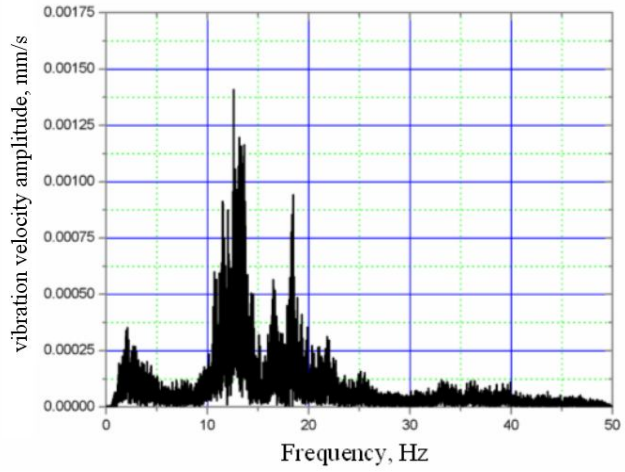


Fig.11. The spectrum of the vibration velocity signal (without air supplying)

ISSN 1313-2539

The measurement point C with the precision carriage being in a static position (with air supplying).

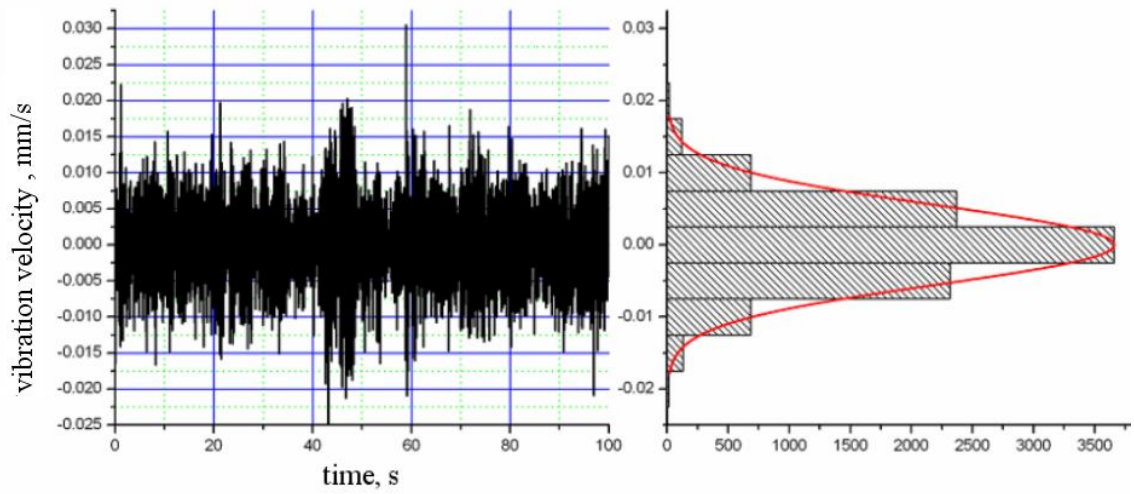


Fig.12. The signal of the vibration velocity and its histogram

Table 3 Statistical parameters of the vibration velocity measurement signal

Statistical parameter	Direction	Arithmetical mean, [mm/s]	Root mean square deviation	Minimum value, [mm/s]	Maximum value, [mm/s]	Scatter, [mm/s]
Point C	horizontal	2.882E-6	0.00549	-0.02623	0.0305	0.05673

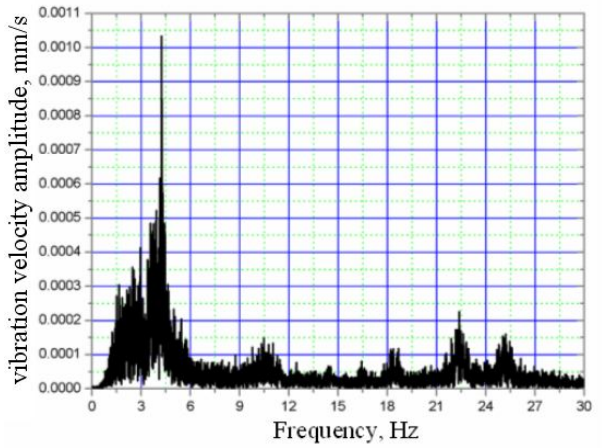


Fig.13. The spectrum of the vibration velocity signal (with air supplying)

The measurement point C during dynamic calibration.

ISSN 1313-2539

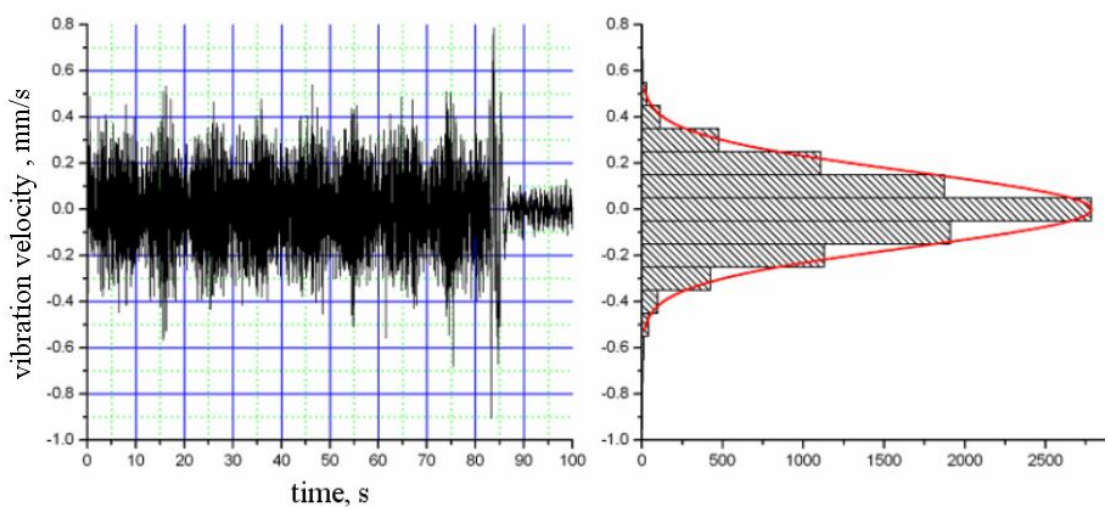


Fig.14. The signal of vibration velocity and its histogram

Table 4 Statistical parameters of the vibrations velocity measurement signal

Statistical parameter	Direction	Arithmetical mean, [mm/s]	Root mean square deviation	Minimum value, [mm/s]	Maximum value, [mm/s]	Scatter, [mm/s]
Point C	horizontal	2.8118E-4	0.16196	-0.90585	0.7869	1.69275

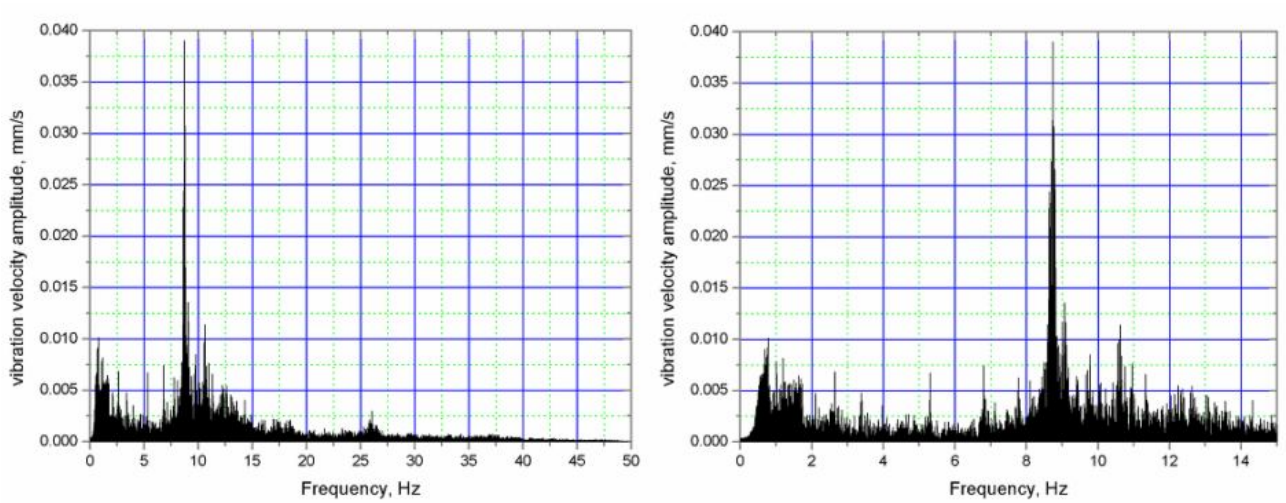


Fig.15. The spectrum of the vibration velocity signal and its fragment (during dynamic calibration)

DISCUSSION OF THE RESULTS

The obtained experimental results show that the spectral amplitudes of the carriage vibrations at 2 – 4 Hz frequencies fluctuate from 0.02 to 0.04 μm, whereas at 10 – 13 Hz frequencies - from 0.02 to 0.025 μm, at 17 – 27 Hz from 0.005 to 0.015 μm, amplitudes at other frequencies are inconsiderable.

Measurements were carried out in horizontal directions. Supply of air to the comparator's frame supports and the carriage's aerostatic bearings was controlled. The illustrations show the measurement point at which vibration velocity amplitudes reach maximum values at the respective frequencies.

ISSN 1313-2539

The obtained experimental results show that the amplitudes of vibration velocity level at 0,1 – 0,4 mm/s (without air supplying) decrease at 0,05 – 0,15 mm/s. The vibration velocities during dynamic calibration fluctuate from 0,2 to 0,4 mm/s. The obtained experimental results show that the spectral amplitudes of vibration velocity (without air supplying) at 10 – 20 Hz frequencies fluctuate from $0{,}5 \cdot 10^{-3}$ to $1{,}4 \cdot 10^{-3}$ mm/s, whereas at other frequencies vibration velocity amplitudes are inconsiderable. The spectral amplitudes of vibration velocity (with air supplying) at 1 – 6 Hz frequencies fluctuate from $0{,}3 \cdot 10^{-3}$ to $1{,}05 \cdot 10^{-3}$ mm/s, whereas at other frequencies vibration velocity amplitudes are inconsiderable. The spectral amplitudes of vibration velocity during dynamic calibration at 8 – 10 Hz frequencies fluctuate from 0,015 to 0,040 mm/s.

Results obtained in theoretical tests are markedly expressed at 10 – 12 Hz frequencies only, where amplitudes reach up to 0,040 mm/s. This is related to inaccurate setting of parameters of differential equations. Hence, result reliability problems arise in the course of determining the vibration level of such accurate calibration devices by calculating methods. Therefore, to find out possible sources of uncertainties and errors in the course of creating tools of such high-end technologies one should be guided by experimental tests despite the fact of their expensive costs.

CONCLUSIONS

1. It has been found out that low-frequency vibrations are capable of affecting the accuracy of reading while the carriage with a microscope are moving.

2. Where the comparator's calibration uncertainty is 0,1 μm/m the obtained values of vibration velocity may affect the accuracy of reading.

3. The spectra of random vibration velocity obtained within the low-frequency range (2 – 10 Hz) define the preparation requirements of the vibration-proof supports.

4. These vibration velocities are acting and must be measured setting the accuracy of raster indication.

REFERENCES

1. Thalmann, R: *A new High Precision Length Measuring Machine, Progress in Precision Engineering and Nanotechnology* (Proceedings of the 9-IPES/UME4, Braunschweig, Germany, 1997, Vol.1, pp. 112-115).

2. F. C. Demarest: *High-resolution, high-speed, low data age uncertainty, heterodyne displacement measuring interferometer electronics* (Meas. Sci. Technol. 9 (1998), P. 1024-1030).

3. J. S. Beers, W. B. Penzes: *The NIST Length Scale Interferometer* (J. Res. Natl. Inst. Stand. Technol. 104, 225 (1999)).

4. NANO 3: *Line Scale Standards, WGDM-7, Preliminary comparison on nanometrology according to the rules of CCL key comparisons* (FINAL REPORT, Braunschweig, August 29, 2003, p. 119).

5. Nano4: *1D gratings, WGDM-7: Preliminary comparison on nanometrology according to the rules of CCL key comparisons* (Final report, Draft B, Wabern, 30. November 2000, p. 34).

6. *Creation and Research into Precision Length Calibration Systems* (2003 Report on the VMSF Research Program Reg. No B-03008, Kaunas 2003, p. 181).

7. *EUROMET Guidelines on Conducting Comparisons EUROMET* (Guide No 3 Issued: 08.12.1998 Revised: 08.05.2002/Sa Version: 02.7b, p.6).

8. EUROMET Guidelines on Conducting Comparisons

ISSN 1313-2539

9. Vibrations in engineering. //Reference book in 6 volumes. Vol. 1/ Edited by V.V. Bolotin, M.: Machine-building, 1978, 352 p.

10. A. Kilikevičius, V. Vekteris: *Vibrations Sources Acting the Comparator Stand* (Mechanika 2006 Proceedings of the 11th international conference. Kaunas 2006).

11. A.Kilikevičius, V. Vekteris: *Diagnostic testing of the comparator carriage vibrations* (Ultragarsas Nr. 2(59). 2006).

12. V. Vekteris, A. Kilikevičius: *Research of vibrations acting the mechatronical comparator* (Zbornik 4. simpozijuma sa medunarodnim učeščem „KOD 2006“ Zbornik Radova Proceedings. Palič 2006).

13. Kasparaitis, V. Vekteris, A. Kilikevičius: *A Vibration Source in Comparator* (Seventh International Conference on Vibration Measurements by Laser Techniques: Advances and Applications Vol.6345. Ancona, Italy, 2006).